Molecular fingerprint of soil organic matter as an indicator of pedogenesis processes in Technosols

Grégoire Pascaud[1] · Marilyne Soubrand[1] · Laurent Lemee[2] · Joëlle Laduranty[2] · Amelène El-Mufleh[2] · Marion Rabiet[1] · Emmanuel Joussein[1]

Abstract

Purpose Technosol management is one of the greatest challenges for the future, more specifically as regards supporting and/or restoring ecosystems. The understanding of natural soil organic matter (SOM) dynamic from Technosol may give important information about soil functioning and Technosol evolution.

Materials and methods According to this, SOM from three French old mine Technosols, (an old tin mine, a lead and zinc, and a gold one which is arsenic-rich), were studied and characterized using thermochemolysis coupled with gas chromatography and mass spectrometry (GC-MS) with tetramethyl ammonium hydroxide (TMAH) as reagent and FTIR. The characterization and quantification of some specific biomacromolecules, used as biomarkers, indicate the specific level of incorporation relative to various subgroups. Global parameters of soils (pH, total organic matter, cation exchange capacity…) were also evaluated.

Results and discussion Results on bulk samples show that lipids are the most reactive group and therefore play the most important role in young soil pedogenesis. All of the results show that the behavior of SOM of the Technosol is similar to homolog non-anthropized soil and depends on vegetation type.

Conclusions A slight inhibition of bacterial activity is observed which underlines a protective effect of Technosols on SOM degradation due to the low pH, the high clay content, and the presence of Al^{3+} and metal(loid)s. In fine, lipid fraction of SOM may act as a well-done fingerprint of pedogenesis processes in Technosols.

Keywords Biomarkers · Py-GC-MS · Soil organic matter · Technosols · Thermochemolysis

1 Introduction

Technosols represent soils subject to strong anthropogenic pressure and particularly to soil influenced by human-made or transformed materials. In this context, mining anthropogenic soils from old abandoned mine zones are spreading (Shrestha and Lal 2011; Mukhopadhyay et al. 2014) and contain a large amount of transformed waste materials often enriched with metals and/or metalloids, thus inducing potential harm to living organisms (Pascaud et al. 2014, 2015; Kumar et al. 2014).

Actually, it is well-known that the natural evolution of Technosols (pedogenesis) may induce the change in contaminant behavior in terms of stability of bearing phases, modification of pH oxydo-reduction conditions, organic matter turnover, change in permeability, or influence of vegetation cover. In fine, the artificialization exerts a direct impact on natural soils by changing both their primary functions and types (from "natural" soils to Technosols). Little is known about Technosol function because of their early development and their low economical attractiveness. As expected in the recent review paper of Leguedois et al. (2016), the understanding of the evolution of Technosols (including mine Technosols) and

the processes involved is an important step necessary for cognitive, applied, and communication goals.

The soil organic matter (SOM) in soil is composed of a heterogeneous fraction of organic compounds (Naafs et al. 2004; Sleutel et al. 2008; Wiesenberg et al. 2012; Huot et al. 2014) such as untransformed molecules like plant residues and microbial compounds, or transformed molecules resulting from biological degradation (De la Rosa et al. 2012; González-Pérez et al. 2012; Carr et al. 2013). This large molecular panel is very complex since it consists of several chemical compound groups as lignin, carbohydrates, proteins, sterols, stanols… and closely depending on the soil specificity. In this way, in a reverse vision, the SOM chemical composition can be a revelator of soil functioning. Indeed, the SOM improves the soils functions by supporting some ecosystems services like water retention, purification, nutriment storage, and carbon sequestration (Janzen 2004). Recently, Huot et al. (2014) have demonstrated that the SOM study can provide potential historical indications to be archived as well as information relative to the contemporary soil organic matter dynamic and soil biological activity (Marseille et al. 1999; Nierop et al. 2005). So the use of molecular marker may provide information on the origin and the degradation rate of organic compounds and in fine onto soils functioning even in the Technosol's early stage formation. According to this fact, the information on SOM transformation offers the keys for the understanding of Technosol evolution.

So, the aims of this paper are to study the global humification rate and way of mine Technosols by fine molecular characterization specially focusing on free lipids as vegetal input tracers or biological biomarkers. Indeed, in the case of contaminated anthropogenic soils for a remediation point of view, the control of influential factors related to the SOM maturation will optimize the settings to improve the biological soil function. The finality of this work is to determine a fingerprint tool for Technosol pedogenesis processes. To do this, it is proposed to focus onto mine soils (i.e., derived from mining wastes) as a Technosol model with significant ecosystem functions even the presence of metallic contamination. Three French contaminated Technosols from abandoned mines (a old tin mine, a lead and zinc, and a gold one which is arsenic-rich) were sampled and characterized according classical pedological investigations (cation exchange capacity (CEC), pH, total organic matter (TOC), total nitrogen (TN), C/N, Al^{3+}, grain size distribution) for the solum positioning according to current pedological concepts. Next, the SOM dynamic has been investigated at the global and the molecular scales using respectively attenuated total reflectance Fourier transform infrared spectroscopy (ATR-FTIR) and thermochemolysis-GC-MS. The latter was applied on both bulk soil and lipid extracts. At last, the general Technosol SOM fingerprint has been compared to the natural soils.

2 Materials and methods

2.1 Site localization and background on soil properties

The studied mining sites were selected according to their geochemical background and equivalent vegetation cover. The majority of former French mines are located on an acidic bedrock basement corresponding to old mountainous massifs like the Armorican Massif, and the Central massif. The three distinct sites herein were chosen for having mined Pb, Sn, and Au in an acidic substrate. In order to compare Technosol development under the same conditions, all the profiles were sampled only on land with minimal slope. High slopes often prove to be unstable and prone to erosion, which in turn induces soil rejuvenation and limits plant growth (Osman and Barakbah 2011). "Natural" plant recolonization was spontaneously established on all study sites. Regardless of the site, a significant presence of birch and brambles was observed, along with sparse shrub and tree growth and, at times, grass growth. As regards the climate parameter, these sites all lie below 750 m in altitude, and their average temperatures correspond to a general oceanic climate pattern (i.e., between 10 and 15 °C over the year).

The localization of the three different sites studied herein is presented in Fig. 1; they have been referenced: Abbaretz ("ABZ"), Mioche ("MCH") and La Petite Faye ("LPF"). The physicochemical characteristics of each soil sample are reported in Table 1. In succinct terms, Abbaretz (ABZ) is an old tin mine located onto a carboniferous quartz vein of the Armorican massif. The soil there has developed on an old sedimentation basin with a water table near 25 cm, and the vegetal cover corresponds to a tall leafy forest. The representative soil profile is shown in Fig. 1. According to the physicochemical properties (Table 1) and redox traces, this anthropogenic acidic soil (pH from 4.1 to 4.9) presents characteristics of Redoxisol for the RP 2008 classification (AFES, 2008) and as Stagnosol for the 2014 WRB (World Reference Base for Soil Resources) classification.

Mioche (MCH) is located in the French Massif Central region and originates from a former lead and zinc mine operating on a granitic basement. The soils were developed on mine tailings, and the sparse vegetation corresponds to an intermediate zone with few deciduous trees (birch) and some lichens. The physicochemical properties and representative soil profile are displayed in Table 1 and Fig. 1, respectively. This anthropogenic acidic soil (low pH ranging from 4.1 to 4.4) shows a high Al^{3+} concentration in the C horizon and a large grain size. Consequently, this soil exhibits characteristics of Alocrisols (Cambisols) and Arenosols (RP and WRB terms, respectively).

The "La Petite Faye" (LPF) samples stem from a former gold mine and have been described previously (Ollivier et al. 2012; Wanat et al. 2014). These soils have been developed
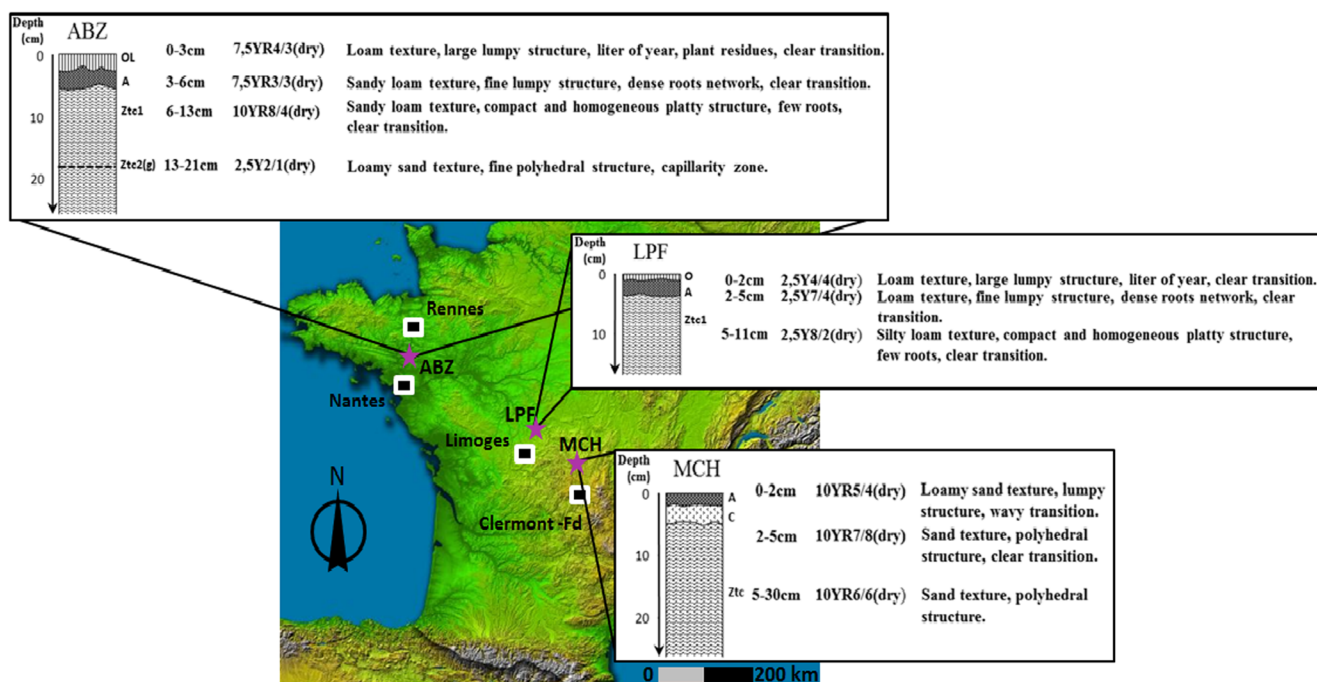
Fig. 1 French selected mine sites and profile presentation

from highly contaminated sediment stored in a settled basin. The well-developed vegetation is composed of deciduous trees, predominantly birch, oak, chestnut and beech, and dense grassland. The presence of paracrystalline materials such as ferrhydrite (8 %), in addition to an acidic pH (3.4 to 4.4) and low density (see Table 1 and Fig. 1) illustrate the andic properties of this soil.

2.2 Sample collection and pedological analysis

The representative profile was selected during every campaign. Each soil horizon was sampled, air-dried, and then sieved to 2 mm before analysis.

The <2 mm fraction of the particle size distribution was determined by sieving and stokes method after organic matter destruction (NF X 31–107). The soil pH was measured with a solid to liquid ratio of 1:5 in double deionized water (according to the NF ISO 10390 Standard). The CEC was determined by the 0.05-N cobaltihexamine method at the soil pH (NF ISO 31–130 Standard). Both TOC and TN were evaluated by means of dry combustion.

Double deionized water (18.2 MΩcm^{-1}) was used for all experiments. All reagents were of analytical grade or higher purity.

2.3 Chemical analysis

Total metal(loid) contents were determined by X-ray fluorescence analyses (XRF) using an XMET 5100 marketed by Oxford Instruments after preparation of pressed pellets.

2.3.1 Characterization of soil organic matter

Molecular analyses were performed on both bulk and lipid fractions.

The lipid fraction from each horizon was extracted from the bulk sample with dichloromethane/methanol (2/1) using a Speed Extractor (Büchi) running at 80 °C, 50 bar, and with a 5-min contact time.

After solvent evaporation, 1 mg of lipids was moistened with a 15 μL tetramethyl ammonium hydroxide (TMAH) solution and then placed in a stainless steel cup prior to thermochemolysis at 400 °C, as will be described hereafter.

The pyrolyzer was a Frontier Lab EGA 2020 model equipped with an AS-1020E auto-shot sampler, coupled with gas chromatography and mass spectrometry (GC-MS Shimadzu QP 2010 Ultra). GC separations were performed using an SLB-5MS (Supelco) capillary column (30 m long, 0.25-mm inner diameter, 0.25-μm phase thickness). The injector temperature was set at 250 °C, while the column temperature was programmed from 50 to 300 °C min^{-1} at a rate of 5 °C m^{-1} and held at 300 °C for 9 min. The ionization mode was electron impact (70 eV) and the source temperature equaled 220 °C.

Thermochemolysis of the bulk fraction was performed at 400 °C (isothermal) using TMAH 50/50 *v/v* in methanol as the alkylating agent. Three milligrams of soil were mixed with 15 μL of TMAH methanolic solution and placed in a stainless steel cup introduced into the auto-shot sampler. The compounds were identified on the basis of their GC retention times and through comparison of their mass spectra with those of reference compounds and of the NIST library,

Table 1 Organic bulk soil characteristics and relative percentages of the various classes of compounds identified in the bulk sample pyrograms (results expressed in %: peak area/$\sum$ peak areas)

	Horizon	Depth	TOC	TN	C/N	Free lipids	% (MO)	pH (H2O)	CEC	Al³⁺	Texture	Lignin	Proteins	Carbohydrate	Fatty acids	Sterols
		cm	g kg⁻¹	g kg⁻¹	–	g kg⁻¹			cmol kg⁻¹	cmol kg⁻¹	%	%	%	%	%	%
ABZ	OL	0–3	292.8	1.5	19.9	47.3	9.4	4.9	ND	ND	ND	34.1	2.4	7.5	55.3	0.8
	A	3–6	164.0	8.7	18.7	24.1	8.5	4.9	16.0	0.17	Silt	29.6	3.6	4.7	61.7	0.4
	Ztc1	6–13	6.7	0.8	8.8	6.1	52.9	4.1	1.8	0.57	Loam clay	5.5	0.1	2.3	92.1	0.1
	Ztc2(g)	13–21	0.5	0.1	3.9	0.2	23.3	4.5	1	0.05	Loamy sand	0.3	0.0	1.3	98.0	0.3
MCH	A	0–2	65.8	4.6	14.3	4.4	3.9	4.4	9.8	0.77	Loamy	26.7	3.5	11.2	58.0	0.6
	C	2–5	2.3	0.2	13.8	0.7	17.7	4.1	4.6	3.15	Sandy	0.4	0.1	0.1	99.0	0.4
	Ztc	5–30	1.2	0.1	9.7	0.4	19.4	4.2	2.0	0.84	Sand	4.3	0.3	0.4	92.3	2.6
LPF	OL	0–2	181.0	18.7	9.7	22.5	7.2	4.4	ND	ND	ND	31.0	3.9	10.5	53.4	1.1
	A	2–5	96.6	13.7	7.1	1.3	0.8	3.8	8.8	0.10	Silty loam	8.2	0.2	5.5	85.4	0.7
	Ztc1	5–11	8.2	1.4	5.8	0.4	2.8	4.3	2.1	0.70	Silty loam	1.0	0.6	0.0	96.1	2.3
	Ztc2	11–15	4.9	1.4	3.4	0.5	5.9	3.4	2.7	1.70	Silty loam	0.2	0.1	0.3	99.1	0.2

TOC total organic carbon, *TN* total nitrogen, *ND* not determined

Attenuated total reflectance Fourier transform infrared spectroscopy ATR-FTIR

ATR-FTIR spectra of the lipid extracts were recorded on a Thermo Fisher Scientific 380 infrared spectrometer (Nicolet) equipped with a diamond crystal. The IR spectra were recorded over a range of 400–4000 cm⁻¹ with a resolution of 4 cm⁻¹. Sixteen scans were collected per spectrum. The atmospheric CO_2 contribution was removed with a straight line between 2400 and 2280 cm⁻¹. Then, spectra were baseline corrected and normalized.
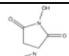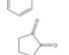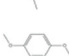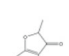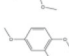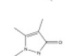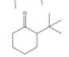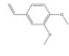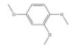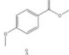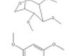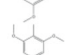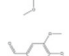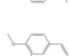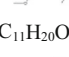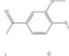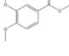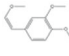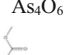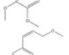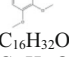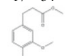
3 Results and discussion

3.1 General characterization of SOM

The global characteristics of the soils such as C to N ratio, TOC, TN, free lipid contents, and pH(H2O) are summarized in Table 1. TOC values decreased with depth for all soil samples, ranging from 292.8 to 0.5 g kg⁻¹ for ABZ, 65.8 to 1.2 g kg⁻¹ for M and 181.0 to 4.9 g kg⁻¹ for LPF. This finding is due to soil organic matter being incorporated along the soil profile (Wiesenberg et al. 2012). TN values also decreased with depth (from 18.7 g kg⁻¹ for LPF to 0.1 g kg⁻¹ for ABZ and MCH). The C to N ratios of soil samples range from 19.9 to 3.9 for ABZ, 14.3 to 9.7 for MCH, and 9.7 to 3.4 for LPF (Table 1), these values are in agreement with data in the literature (Matus et al. 2014; Santana et al. 2015) and could suggest an increase of decomposition of plant-derived compounds.

In the way to better characterize SOM in a structural point of view, thermochemolysis-GC-MS of bulk samples was done. The various compounds produced are reported in Table 2. These compounds are characteristic of five distinct origins, respectively, lignin, proteins, carbohydrate, fatty acids, and steroids. Alkylbenzenes and phenolic compounds (as methyl ethers) result from the thermal degradation of lignin. Nitrogen-containing compounds originate from proteins, whereas the thermochemolysis of cellulose produces furans and glucose (Table 2). Fatty acids are detected as methyl esters in the C_{15}–C_{32} range. Steranes and a steroidic ketone originating from sterols could be detected. Moreover, a by-product of the arsenic-bearing phase was detected for the LPF profile (molecule no. 23 in Table 2); its presence suggests that the thermochemolysis of a highly contaminated soil in As may induce the occurrence of oxides such as As_4O_6, which naturally bias the organic compound quantification. This compound seems to appear during thermochemolysis after recombination between As and O in the oxidant pyrolyzer condition. To avoid this bias, compound no. 23 will not be taken into consideration during the quantification. This method, associated with the molecular chain summarized in Table 2, has been devised in accordance with the surface horizons for these three soil profiles. This relative quantification therefore enables
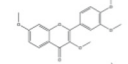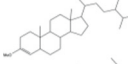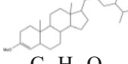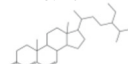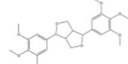
Table 2   Pyrolysis products of bulk samples

n°	Name	Molecular weight g.mol^{-1}	RT min	Structure	Origin
1	Hydroxy pyrrolidinedione	115	10.19		P
2	Hydroxyethyl methyl pyrazolinone	142	11.34		P
3	Benzoic acid methyl ester	136	12.08		C
4	Methyl cyclopentanedione	112	12.25		C
5	Dimethoxy benzene	138	14.09		L
6	Methoxy dimethyl furanone	142	15.81		C
7	Dimethoxytoluene	152	16.21		L
8	Ethyl dimethyl pyrazolinone	154	16.38		P
9	Tertabutylcyclohexanone	154	19.17		F
10	Ethenyl dimethoxy benzene	164	19.76		L
11	Trimethoxybenzene	168	19.86		L
12	Methoxy benzoic acid methyl ester	135	20.07		L
13	1.6-Anhydro-⊠ D-glucose trimethyl ether	101	20.27		C
14	Trimethoxy benzene	168	20.94		L
15	Trimethoxytoluene	182	22.73		L
16	Dimethoxy benzaldehyde	166	22.87		L
17	Dimethoxy propenyl benzene	178	23.10		L
18	Nonanedioic acid dimethyl ester	216	24.20	$C_{11}H_{20}O_4$	F
19	Dimethoxyphenyl ethanone	165	24.87		L
20	Dimethoxy benzoic acid methyl ester	196	25.44		L
21	Dimethoxy methoxyethenyl benzene	194	26.21		L
22	Dimethoxy methoxyethenyl benzene	194	26.52		L
23	Hexaoxa tetraarsatricyclo decane	396	27.07	As_4O_6	*
24	Propenoic acid methoxyphenyl methyl ester	192	27.45		L
25	Trimethoxy benzoic acid methyl ester	226	28.24		L
26	Dimethoxy (methoxy propenyl) benzene	208	28.74		L
27	*Iso* pentadecanoic acid methyl ester	256	29.59	$C_{16}H_{32}O_2$	F
28	*Anteiso* pentadecanoic acid methyl ester	256	29.75	$C_{16}H_{32}O_2$	F
29	Pentadecanoic acid methyl ester	256	30.37	$C_{16}H_{32}O_2$	F
30	Heptadecanone	254	30.74	$C_{17}H_{34}O$	F
31	Branched hexadecanoic acid methyl ester	268	31.66	$C_{17}H_{34}O_2$	F
32	Dimethoxyphenyl propenoic acid methyl ester	222	31.82		L

Origin: P proteins, C carbohydrate, L lignine, F fatty acid, S sterols

*Pyrolysis by-product of As bearing phase

Table 2 (continued)

n°	Name	Molecular weight g.mol^{-1}	RT min	Structure	Origin
33	Hexadecenoic acid methyl ester	268	31.99	$C_{17}H_{32}O_2$	F
34	Hexadecenoic acid methyl ester Z	268	32.18	$C_{17}H_{32}O_2$	F
35	Hexadecanoic acid methyl ester E	270	32.43	$C_{17}H_{34}O_2$	F
36	Heptadecenoic acid methyl ester	282	34.35	$C_{18}H_{34}O_2$	F
37	Octadecenoic acid methyl ester Z	296	35.74	$C_{19}H_{36}O_2$	F
38	Octadecenoic acid methyl ester E	296	35.85	$C_{19}H_{36}O_2$	F
39	Octadecanoic acid methyl ester Z	298	36.23	$C_{19}H_{38}O_2$	F
40	Octadecadienoic acid methyl ester	294	36.58	$C_{19}H_{34}O_2$	F
41	Octadecenoic acid methyl ester Z	296	36.74	$C_{19}H_{36}O_2$	F
42	Hexadecanoic diacid methyl ester	314	38.49	$C_{18}H_{38}O_4$	F
43	Eicosanoic acid methyl ester	326	39.73	$C_{20}H_{38}O_2$	F
44	Uncosanoic acid methyl ester	340	41.37	$C_{21}H_{40}O_2$	F
45	Docosanoic acid methyl ester	354	42.95	$C_{22}H_{42}O_2$	F
46	Methoxy nonadecanoic acid methyl ester	342	43.39	$C_{21}H_{42}O_3$	F
47	Tricosanoic acid methyl ester	368	44.45	$C_{23}H_{44}O_2$	F
48	Heptacosane	380	45.46	$C_{27}H_{56}$	F
49	Tetracosanoic acid methyl ester	382	45.93	$C_{24}H_{46}O_2$	F
50	Methoxy uncosanoic acid methyl ester	370	46.39	$C_{23}H_{46}O_3$	F
51	Methoxy C16	372	47.32	$C_{16}H_{29}O_3$	F
52	Docosanoic diacid methyl ester	398	47.79	$C_{24}H_{46}O_4$	F
53	Nonacosane	408	48.24	$C_{29}H_{60}$	F
54	Hexacosanoic acid methyl ester	410	48.71	$C_{26}H_{48}O_2$	F
55	Methoxy tricosanoic acid methyl ester	398	49.13	$C_{25}H_{50}O_3$	F
56	Methoxy C18	414	49.99	$C_{18}H_{33}O_3$	F
57	Octacosanoic acid methyl ester	438	51.32	$C_{28}H_{50}O_2$	F
58	Dimethoxyphenyl dimethoxy-benzopyranone	342	51.89		L
59	β- methoxy stigmastane	428	53.30		S
60	α-methoxy stigmastane	428	53.30		S
61	Tricontanoic acid methyl ester	466	54.29	$C_{30}H_{52}O_2$	F
62	Stigmastadiene-3-one	410	55.57		S
63	1H.3H-Furo[3.4-c]furan.tetrahydro-1.4-bis(3.4.5-Trimethoxyphenyl)-.[1S-(1.α.3a.α.4.α.6a. α)]-	446	58.03		L
64	Dotricontanoic acid methyl ester	494	58.37	$C_{32}H_{56}O_2$	F

comparing the SOM repartition at these three study sites. The range of relative group contents (expressed in % and calculated as follows: peak area/$\sum$ peak areas) is presented in Table 1.

Fatty acids are the two main identified thermochemolysis products. In contrast, steroids are detected as trace components. The lignin percentages decrease from top to bottom of the ABZ profile, respectively, from 34.1 to 0.3 %. This trend seems to be nonlinear, with a strong decrease appearing between the A and Ztc1 horizons (29.6 to 5.5 %). This same trend is observed for protein fragments, whereas the cellulose and sterol compound proportions show a linear decrease from top to bottom (from 7.5 to 1.3 %). In contrast, the relative proportions of fatty acid compounds increase with depth from 55.3 % for the OL horizon to 98 % in Ztc2(g). Similar trends are obtained in the case of MCH and LPF soil profiles for the lignin, protein, cellulose, and fatty acid class components.

Carbohydrate-derived products, however, are less mobilized than the ABZ soil profile (Table 1).

On a global scale, the vertical repartition of SOM seems to be similar for all origins. Lignin, proteins, and carbohydrate are poorly incorporated over the soil depth, which is in agreement with the literature (Jenkinson and Coleman 2008; Thevenot et al. 2010; Carr et al. 2013). This fresh vegetal organic matter is poorly incorporated in soils, whereas fatty acids and sterols (i.e., the lipids; Quenea et al. 2004; de Blas et al. 2013) are more readily incorporated. In fine, the lipids correspond to the mobile and biodegradable fractions which decrease with depth (Celerier et al. 2009). The migration of lipid in the studied soils can be linked to the lower pH values (see Table 1; pH values from 4.9 for ABZ to 3.4 for LPF in the Ztc horizon) which increase their mobility (Nierop et al. 2005). On the other hand, the low pH values could not explain

the large family migration differences from one profile to the next (e.g., cellulose incorporation in the ABZ profile, differences in sterol behavior).

It is therefore obvious that other setting parameters are capable of greatly affecting organic compound incorporation; these parameters include the following: (i) physicochemical properties such as particle size fractions (texture) and pH values of soils (Quenea et al. 2004; Aciego Pietri and Brookes 2008), (ii) soil toxicity towards microbiological life and biological activity (Naafs et al. 2004), (iii) vegetation cover type (De la Rosa et al. 2012; de Blas et al. 2013), and (iv) the SOM structure. This latter behavior can be ascribed to the difference in texture. Indeed, the high clay content observed in mine Technosols (ABZ and LPF) can sometimes increase SOM stability via sorption or complexation (Naafs et al. 2004; O'Brien and Jastrow 2013). Moreover, for ABZ Technosol, this behavior can also be explained by the change of redox conditions due to the water table flapping (Ztc1–Ztc2(g)) with periods of saturation and desaturation one. It has been demonstrated that redox conditions promote the solubilization of SOM (Grybos et al. 2009; Hanke et al. 2014). In our case, either SOM is being leached after solubilization, which would explain the decrease of lipid % in Ztc2(g) (ABZ), or Ztc1 is being enriched by capillary rise.

Due to their reactivity with the mineral sphere, lipid bioavailability and mobility at the profile scale are reduced by the mine Technosol background (i.e., a large volume of clays, fine material fractions, water conditions), yet it is obvious that these lipids play a major role in the SOM dynamic; consequently, the finest characterizations yield information on origin and decomposition type.

3.2 The lipid fraction as a tracer of the SOM origin

The lipid fraction was extracted and characterized using ATR-FTIR and thermochemolysis-GC-MS pyrolysis; these results are listed in Fig. 2 and Table 3, respectively. The infrared spectra (Fig. 2a–c) of lipids for each soil profile reveal the various functional groups present with depth. Regardless of the soil profile, the bands localized at 2920 and 2850 cm^{-1} are correlated with the aliphatic group (alkanes) stretching band, confirmed by a deformation band at 1460 and 1370 cm^{-1}. The 750 cm^{-1} band is due to the ortho-substituted aromatic compounds (stretching band). Aliphatic carboxylic acids have also been identified by the band at 1710 cm^{-1}, corresponding to the C = O carboxylic acid vibration. Furthermore, a shoulder at 1730 cm^{-1} is attributed to ketones.

A comparison of the various spectra provides some information about the incorporation of fresh soil organic matter. Independent of the soil profile, no evolution can be observed in the aliphatic group (alkanes) and aliphatic carboxylic acids with depth (see Fig. 2). These differences are significant for the aromatic compounds (with a band at 750 cm^{-1}) and
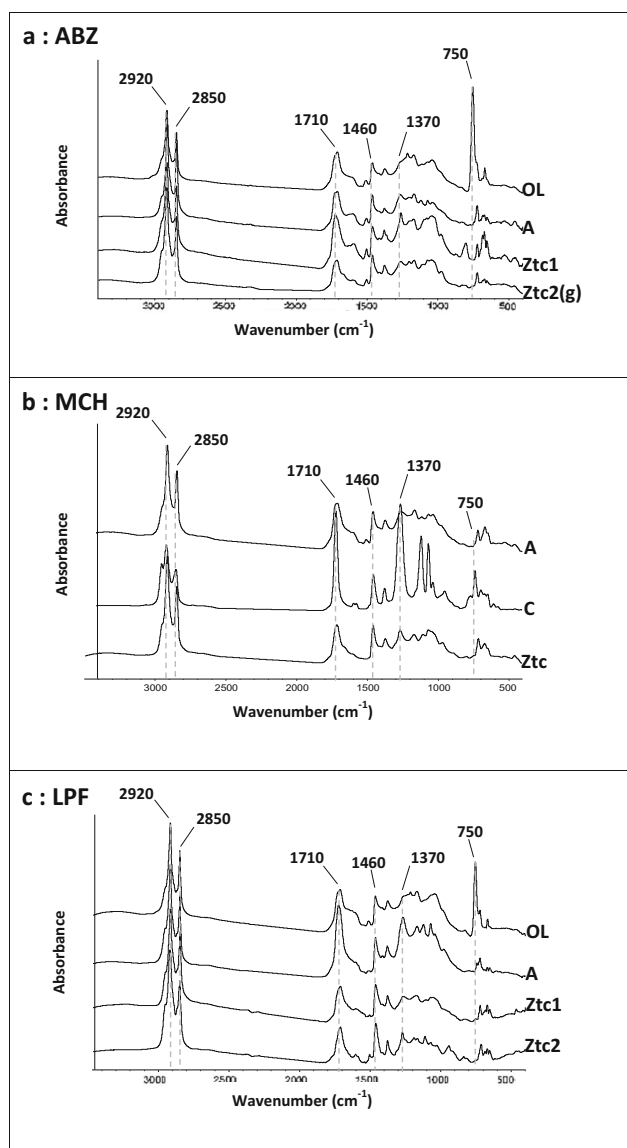
Fig. 2 Attenuated reflectance infrared spectra of the Technosol lipid fraction

decrease with depth. Such trends are highly visible for both the ABZ and LPF profiles (Fig. 2 a, c) and, to a lesser extent, for the MCH profile (Fig. 2b). These results can be explained by the absence of an OL horizon in the MCH soil profile compared to the ABZ and LPF profiles (where the OL horizons are present). The FTIR exposes the SOM evolution at the profile scale and with respect to the functional group. To better understand the SOM dynamic and evolution, refined techniques are implemented to characterize the lipid fraction as needed. The thermochemolysis products of lipid fractions are listed in Table 3.

Fatty acids (detected as methyl esters) are the main compounds, as observed in the thermochemolysis products of lipid fractions. Several minor series, like hydroxy acids detected as

Table 3 Pyrolysis products of the lipid fractions

n	Name	Correspondence methylated compound	Molecular weight g mol^{-1}	RT min	Structure
1	Nonanedioic acid dimethyl ester	Nonanedioic acid, dimethyl ester	216	24.2	$C_{11}H_{20}O_4$
2	Iso pentadecanoic acid methyl ester	C_{15}Me iso	256	29.59	$C_{16}H_{32}O_2$
3	Anteiso pentadecanoic acid methyl ester	C_{15}Me anteiso	256	29.75	$C_{16}H_{32}O_2$
4	Pentadecanoic acid methyl ester	C_{15}Me	256	30.37	$C_{16}H_{32}O_2$
5	Heptadecanone	KetoneC_{17}	254	30.74	$C_{17}H_{34}O$
6	Branched hexadecanoic acid methyl ester	C_{16}Me branched	268	31.66	$C_{17}H_{34}O_2$
7	Hexadecenoic acid methyl ester	$C_{16:1}$Me	268	31.99	$C_{17}H_{32}O_2$
8	Hexadecenoic acid methyl ester Z	$C_{16:1}$Me	268	32.18	$C_{17}H_{32}O_2$
9	Hexadecanoic acid methyl ester E	C_{16}Me	270	32.43	$C_{17}H_{34}O_2$
10	Heptadecenoic acid methyl ester	C_{17}Me	282	34.35	$C_{18}H_{34}O_2$
11	Octadecenoic acid methyl ester Z	$C_{18}:1$Me	296	35.74	$C_{19}H_{36}O_2$
12	Octadecenoic acid methyl ester E	$C_{18}:1$Me	296	35.85	$C_{19}H_{36}O_2$
13	Octadecanoic acid methyl ester Z	C_{18}Me	298	36.23	$C_{19}H_{38}O_2$
14	Octadecadienoic acid methyl ester	$C_{18:2}$Me	294	36.58	$C_{19}H_{34}O_2$
15	Octadecenoic acid methyl ester Z	$C_{18:1}$Me	296	36.74	$C_{19}H_{36}O_2$
16	Hexadecanoic diacid methyl ester	DiC_{16}Me	314	38.49	$C_{18}H_{38}O_4$
17	Eicosanoic acid methyl ester	C_{19}Me	326	39.73	$C_{20}H_{38}O_2$
18	Uncosanoic acid methyl ester	C_{20}Me	340	41.37	$C_{21}H_{40}O_2$
19	Docosanoic acid methyl ester	C_{21}Me	354	42.95	$C_{22}H_{42}O_2$
20	Methoxy nonadecanoic acid methyl ester	methoxyesterC_{19}	342	43.39	$C_{21}H_{42}O_3$
21	Tricosanoic acid methyl ester	C_{22}Me	368	44.45	$C_{23}H_{44}O_2$
22	Heptacosane	AlkanC_{27}	380	45.46	$C_{27}H_{56}$
23	Tetracosanoic acid methyl ester	C_{23}Me	382	45.93	$C_{24}H_{46}O_2$
24	Methoxy uncosanoic acid methyl ester	methoxyesterC_{21}	370	46.39	$C_{23}H_{46}O_3$
25	Methoxy C_{16}	methoxyC_{16}	372	47.32	$C_{16}H_{34}O$
26	Docosanoic diacid methyl ester	DiC_{22}Me	398	47.79	$C_{24}H_{46}O_4$
27	Nonacosane	AlkanC_{29}	408	48.24	$C_{29}H_{60}$
28	Hexacosanoic acid methyl ester	C_{26}Me	410	48.71	$C_{26}H_{48}O_2$
29	Methoxy tricosanoic acid methyl ester	methoxyesterC_{23}	398	49.13	$C_{25}H_{50}O_3$
30	Methoxy C_{18}	methoxyC_{18}	414	49.99	$C_{18}H_{38}O$
31	Octacosanoic acid methyl ester	C_{28}Me	438	51.32	$C_{28}H_{50}O_2$
32	Beta methoxy stigmastane	beta methoxy stigmastane	428	53.30	$C_{30}H_{52}O$
33	Alpha methoxy stigmastane	alpha methoxy stigmastane	428	53.30	$C_{30}H_{52}O$
34	Tricontanoic acid methyl ester	C_{30}Me	466	54.29	$C_{30}H_{52}O_2$
35	Stigmastadiene-3-one	4,22-Stigmastadiene-3-one	410	55.57	$C_{29}H_{46}O$
36	Dotricontanoic acid methyl ester	C_{32}Me	494	58.37	$C_{32}H_{56}O_2$

methoxy esters, diacids detected as dimethyl esters, alkanes, ketones, and steroids, are also observed.

Fatty acids range from C_{15} to C_{32}, with a bimodal distribution. In the short mode, palmitic (C_{16}) and stearic (C_{18}) acids are ubiquitous; $C_{16:1}$ and $C_{16:2}$ are both correlated with bacteria and fungi (Ruess et al. 2002; Taube et al. 2013); and the branched C_{15} and C_{17} are of microbial origin (Marseille et al. 1999). In the long mode on the other hand, the even-chained compounds are of plant origin, with such a predominance often being observed in a forest or grassland soils (Almendros et al. 1996; de Blas et al. 2013). At the same time,

the presence of straight chain C_{10} through C_{20} is currently associated with the fungal activity/input (Li et al. 2013). The most likely source of n-alkanoic acids in soil corresponds to the plant lipid oxidation derived from vegetation and percolating through the profile along the hydric path (Celerier et al. 2009).

Hydroxy acids (detected as methoxy esters) in addition to diacids C_{16} and C_{22} (detected as diesters) were also observed. α-diacids are of plant origin (cutin and suberin) (Bull et al. 1998) and ω-diacids are related to the terminal oxidization by biological means. In contrast, as regards the monoacid

resemblance, it appears that these substances may be a source of diacids (Celerier et al. 2009).

Alkanes are identified in all three profiles, with predominance for C_{27}. These compounds are not correlated with the bacterial activity; long odd-chained alkanes are traditionally associated with the epicuticular waxes and protective layer in vascular plants. The observed C_{27} and C_{29} hydrocarbons are thus correlated with long-chained fatty acids and originate from plants. On the other hand, these long odd-chained alkanes can also be produced by fungal activity (Bull et al. 1998; Naafs et al. 2004).

Some methoxyester has been detected for the various profiles, ranging from C_{19} to C_{23} with maximization at C_{19}. Their repartition is rather heterogeneous in considering the different profiles; it does not seem to match the vegetal organic matter repartition (i.e. decreasing with depth).

A ketone C_{17} is observed for the profile with a predominance of grassland soils (MCH and LPF). Ketones are produced either after the terminal alkane oxidation or by the fatty acid β-oxidation followed by a decarboxylation (Celerier et al. 2009). In this case, the low alkane content indicates that ketones might be derived from fatty acids; hence the presence of ketones implies in situ microbial oxidation.

Steroids were detected in low quantities, i.e. compounds no. 32, 33 and 35, respectively as β-methoxy stigmastadiene, α-methoxy stigmastadiene C_{30}, and 4.22-stimastadiene-3-one C_{29}. Such a distribution is commonly observed in terrestrial organic matter derived from higher vascular plants (Peters 2005; Fabiańska and Smółka-Danielowska 2012).

Several compound types however may provide an indication of soil functioning, especially the branched C_{15} iso- and anteiso-fatty acids. These molecules are closely correlated

with the microbial activity (Bull et al. 1998). The ratio (isoC$_{15}$ + anteisoC$_{15}$)/C$_{15}$ values are listed in Fig. 3; these values reflect current bacterial activity in the surface horizons and poor activity in the deepest horizon (Celerier et al. 2009): on a global scale, these values range from 3.88 to 0.52. They seem to be lower for the MCH profile: 2.39 to 0.52. The CPI (Carbon Preference Index) values have been gathered in Fig. 3 and range overall from 1.28 to 0.29. Nearly all of these values are less than 1, which highlights the even mod predominance that is indicative of the limited degradation of primary plant biomass (Huot et al. 2014). The LMW/HMW (Low Molecular Weight/High Molecular Weight) ratio provides evidence about the biological activity, with a low molecule corresponding for the most part to microbial or fungal activity. The values observed reveal a peak on the dense root network zone C horizon for M and A of the LPF profile. At the ABZ site, the highest value is associated with the Ztc2(g) horizon; this result may be due to the vegetation characteristic: in this instance, ABZ is under a forest soil. This correlation between roots and fungal activity has been cited in several studies (Madan et al. 2002; Ruess et al. 2002; Mardhiah et al. 2014).

3.3 Comprehensive approach and comparison with natural soils

At first glance, the presence of branched fatty acids and diacids suggests undisturbed soil functioning. However, the CPI molar ratio, which indicates the predominance of even-chained fatty acids (CPI <1), would suggest a low degradation of primary plant biomass (Wiesenberg et al. 2012); in conjunction with this result, C_{15} iso- and anteiso-fatty acids demonstrate that the bacterial activity is more pronounced in the surface horizon than in

Fig. 3 Molar ratio vs. depth
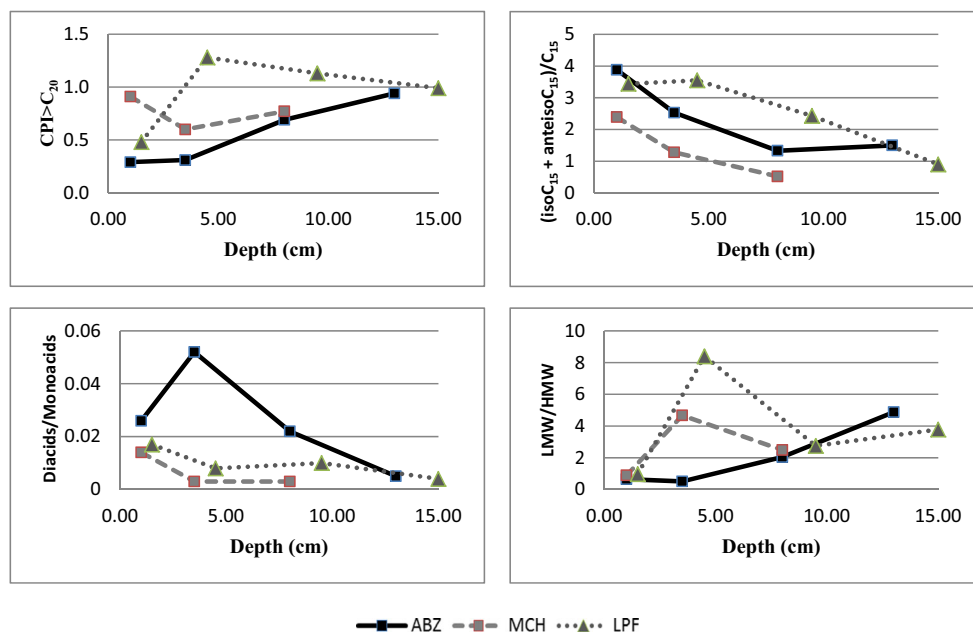
deeper horizons (as is typically observed for natural soils) (Stone et al. 2014). When compared to natural soils however, it would appear that these values are significantly lower (Celerier et al. 2009); moreover, the absence of C_{17} iso- and anteiso-alkanoic acids suggests that bacterial activity is slightly inhibited. These results may be correlated with the acidic soil results; several studies demonstrate the inhibition of bacterial activity under acidic soil conditions: low pH and high free Al contents (Dinel et al. 1990; Parfitt et al. 1999; Naafs et al. 2004; Suárez-Abelenda et al. 2015). In contrast, unlike bacterial activity, the arbuscular myccorhizal fungi seem to be heavily involved in the andic soil functioning (Rillig et al. 2001). In our case, some biomarkers indicate the contribution of fungi (alkanes, methoxy ester repartition), but nothing allows us to conclude that fungal activity is higher or occurs at the expense of bacterial activity.

These biomarkers therefore suggest a slower degradation of SOM in the Technosol profiles, compared to the natural homologous soil; this occurrence might be correlated with the protector characteristic of soil towards SOM against biodegradation (Naafs et al. 2004; Matus et al. 2014). Various mechanisms can be responsible for this phenomenon in natural soils: (i) acidic properties are known to inhibit bacterial activity; (ii) several complexation reactions like organometallic or clay interaction can avoid the biodegradability of SOM by stabilization (Skjemstad et al. 2008; O'Brien and Jastrow 2013; Song et al. 2013) (these stable organometallic and organo-clayey complex formations are exacerbated by the presence of excessive quantities of clays); and (iii) lastly, the free Al toxicity (Naafs et al. 2004). If the slower degradation of SOM can be ascribed to low pH and the mineralogical sequence in the natural soil, then the mine Technosol background implies additional factors that may alter biological activity, like: toxic metal bearing phases, a very fine particle grain size, high clay content, and high free Al content. Metals or metalloids like Al, As, Pb, and Sb are indeed known to be toxic for microbial fauna (Singh et al. 2004; Nayak et al. 2014). In addition, several sorption phenomena have been observed between Al and Fe hydrous oxides (Parfitt et al. 1999) and paracrystalline minerals present in huge amounts, triggering another type of protection in favor of SOM and potentially slowing its fast degradation.

To conclude, the results obtained in this study clearly show that the dynamic of organic matter into the three mine Technosol samples appears to be similar to that of non-anthropized soils (having similar functioning). Moreover, SOM turnover commonly depends on vegetation type as in natural soils (Leguedois et al. 2016). However, it is clear that soil development is slower, in particular due to the low fertility of tailings, their acidic nature, the protective effect on SOM, and their potential toxicity for microbial fauna.

4 Conclusions

The mine Technosols organic matter dynamic by various technics has been studied at three different representative mine sites located on a bedrock basement in the context of future management/remediation point of view.

The results clearly evidenced that the molecular fingerprint of SOM can be a usefool tool as an indicator of pedogenesis processes in Technosols. The SOM seems to follow the vegetal cover type then indicating a main plant input. However, the SOM incorporation and the increase of the bioavailable fraction relative to fertility (and to a greater extent the ecosystem support potential) depend on the biodegradation of fresh natural organic matter. Thus, it appears that the biological (microbial, fungal, and vegetal) activity that plays such a major role in the pedogenesis process is slowed by the mine Technosol background. Calculations with several origin biomarkers extracted from pyrolysis data indicate not only (i) the normal functioning of Technosol compared to a natural homologous soil but also (ii) the carbon dynamic seems to be slowed by the protective effect of Technosol on SOM. It can be hypothesized that this later effect is essentially may be due to low pH of Technosols, the high clay content which may create strong interactions between inorganic and organic matter (and consequently decreasing SOM bioavailability), and the soil toxicity towards microorganisms (presence of Al^{3+} and metal(loid)s).

From a broader perspective, only the understanding, protection, and restoration of soil function will promote ecosystem services. A Technosol management approach will rely on the set of parameters explained above in order to promote the SOM dynamic and, consequently, to perceive the beneficial impacts on fertility and, more specifically, on the potential to support ecosystems.

References

Aciego Pietri JC, Brookes PC (2008) Relationships between soil pH and microbial properties in a UK arable soil. Soil Biol Biochem 40: 1856–1861

Almendros G, Sanz J, Velasco F (1996) Signatures of lipid assemblages in soils under continental Mediterranean forests. Eur J Soil Sci 47: 183–196

Bull ID, van Bergen PF, Poulton PR, Evershed RP (1998) Organic geochemical studies of soils from the Rothamsted classical experiments—II, soils from the Hoosfield spring barley experiment treated with different quantities of manure. Org Geochem 28:11–26

Carr AS, Boom A, Chase BM, et al. (2013) Biome-scale characterisation and differentiation of semi-arid and arid zone soil organic matter

compositions using pyrolysis–GC/MS analysis. Geoderma 200-201:189–201

Celerier J, Rodier C, Favetta P, et al. (2009) Depth-related variations in organic matter at the molecular level in a loamy soil: reference data for a long-term experiment devoted to the carbon sequestration research field. Eur J Soil Sci 60:33–43

De Blas E, Almendros G, Sanz J (2013) Molecular characterization of lipid fractions from extremely water-repellent pine and eucalyptus forest soils. Geoderma 206:75–84

De la Rosa JM, Faria SR, Varela ME, et al. (2012) Characterization of wildfire effects on soil organic matter using analytical pyrolysis. Geoderma 191:24–30

Dinel H, Schnitzer M, Mehuys G (1990) Soil lipids: origin, nature, content, decomposition, and effect on soil physical properties. Soil Biochem 6:397–429

Fabiańska MJ, Smółka-Danielowska D (2012) Biomarker compounds in ash from coal combustion in domestic furnaces (Upper Silesia Coal Basin, Poland). Fuel 102:333–344

González-Pérez JA, Chabbi A, de la Rosa JM, et al. (2012) Evolution of organic matter in lignite-containing sediments revealed by analytical pyrolysis (Py–GC–MS). Org Geochem 53:119–130

Grybos M, Davranche M, Gruau G, et al. (2009) Increasing pH drives organic matter solubilization from wetland soils under reducing conditions. Geoderma 154:13–19

Hanke A, Sauerwein M, Kaiser K, Kalbitz K (2014) Does anoxic processing of dissolved organic matter affect organic–mineral interactions in paddy soils? Geoderma 228-229:62–66

Huot H, Faure P, Biache C, et al. (2014) A Technosol as archives of organic matter related to past industrial activities. Sci Total Environ 487:389–398

Janzen HH (2004) Carbon cycling in earth systems—a soil science perspective. Agric Ecosyst Environ 104:399–417

Jenkinson DS, Coleman K (2008) The turnover of organic carbon in subsoils. Part 2. Modelling carbon turnover. Eur J Soil Sci 59:400–413

Kumar B, Verma VK, Naskar AK, et al. (2014) Bioavailability of metals in soil and health risk assessment for populations near an Indian chromite mine area. Hum Ecol Risk Assess Int J 20:917–928

Leguédois S, Séré G, Auclerc A, Cortet J, Huot H, Ouvrard S, Watteau F, Schwartz C, Morel JL (2016) Modelling pedogenesis of Technosols. Geoderma 262:199–212

Li Y, Liang M, Shu X, et al. (2013) Differentiation of basidiospores by MALDI-TOF lipid profiling. Int J Mass Spectrom 352:44–50

Madan R, Pankhurst C, Hawke B, Smith S (2002) Use of fatty acids for identification of AM fungi and estimation of the biomass of AM spores in soil. Sol Biol Biochem 34:125–128

Mardhiah U, Caruso T, Gurnell A, Rillig MC (2014) Just a matter of time: fungi and roots significantly and rapidly aggregate soil over four decades along the Tagliamento River, NE Italy. Soil Biol Biochem 75:133–142

Marseille F, Disnar JR, Guillet B, Noack Y (1999) N-alkanes and free fatty acids in humus and A1 horizons of soils under beech, spruce and grass in the Massif-Central (Mont-Lozère), France: n-alkanes in soils under beech, spruce and grass. Eur J Soil Sci 50:433–441

Matus F, Rumpel C, Neculman R, et al. (2014) Soil carbon storage and stabilisation in andic soils: a review. Catena 120:102–110

Mukhopadhyay S, Maiti SK, Masto RE (2014) Development of mine soil quality index (MSQI) for evaluation of reclamation success: a chronosequence study. Ecol Eng 71:10–20

Naafs DF, van Bergen PF, Boogert SJ, de Leeuw JW (2004) Solvent-extractable lipids in an acid andic forest soil; variations with depth and season. Soil Biol Biochem 36:297–308

Nayak AK, Raja R, Rao KS, et al. (2014) Effect of fly ash application on soil microbial response and heavy metal accumulation in soil and rice plant. Ecotoxicol Environ Saf 114:257–262

Nierop KGJ, Naafs DFW, van Bergen PF (2005) Origin, occurrence and fate of extractable lipids in Dutch coastal dune soils along a pH gradient. Org Geochem 36:555–566

O'Brien SL, Jastrow JD (2013) Physical and chemical protection in hierarchical soil aggregates regulates soil carbon and nitrogen recovery in restored perennial grasslands. Soil Biol Biochem 61:1–13

Ollivier J, Wanat N, Austruy A, et al. (2012) Abundance and diversity of ammonia-oxidizing prokaryotes in the root–rhizosphere complex of Miscanthus × giganteus grown in heavy metal-contaminated soils. Microb Ecol 64:1038–1046

Osman N, Barakbah SS (2011) The effect of plant succession on slope stability. Ecol Eng 37:139–147

Parfitt RL, Yuan G, Theng BKG (1999) A 13C-NMR study of the interactions of soil organic matter with aluminium and allophane in podzols. Eur J Soil Sci 50:695–700

Pascaud G, Boussen S, Soubrand M, et al. (2015) Particulate transport and risk assessment of Cd, Pb and Zn in a Wadi contaminated by runoff from mining wastes in a carbonated semi-arid context. J Geochem Explor 152:27–36

Pascaud G, Leveque T, Soubrand M, et al. (2014) Environmental and health risk assessment of Pb, Zn, As and Sb in soccer field soils and sediments from mine tailings: solid speciation and bioaccessibility. Environ Sci Pollut Res 21:4254–4264

Peters KE (2005) The biomarker guide, 2nd edn. Cambridge University Press, Cambridge

Quenea K, Derenne S, Largeau C, et al. (2004) Variation in lipid relative abundance and composition among different particle size fractions of a forest soil. Org Geochem 35:1355–1370

Rillig MC, Wright SF, Nichols KA, et al. (2001) Large contribution of arbuscular mycorrhizal fungi to soil carbon pools in tropical forest soils. Plant Soil 233:167–177

Ruess L, Häggblom MM, García Zapata EJ, Dighton J (2002) Fatty acids of fungi and nematodes—possible biomarkers in the soil food chain? Soil Biol Biochem 34:745–756

Santana GS, Knicker H, González-Vila FJ, et al. (2015) The impact of exotic forest plantations on the chemical composition of soil organic matter in Southern Brazil as assessed by Py–GC/MS and lipid extracts study. Geoderma Reg 4:11–19

Shrestha RK, Lal R (2011) Changes in physical and chemical properties of soil after surface mining and reclamation. Geoderma 161:168–176

Singh AN, Raghubanshi AS, Singh JS (2004) Impact of native tree plantations on mine spoil in a dry tropical environment. For Ecol Manag 187:49–60

Skjemstad JO, Krull ES, Swift RS, Szarvas S (2008) Mechanisms of protection of soil organic matter under pasture following clearing of rainforest on an Oxisol. Geoderma 143:231–242

Sleutel S, Leinweber P, Begum SA, et al. (2008) Composition of organic matter in sandy relict and cultivated heathlands as examined by pyrolysis-field ionization MS. Biogeochemistry 89:253–271

Song XY, Spaccini R, Pan G, Piccolo A (2013) Stabilization by hydrophobic protection as a molecular mechanism for organic carbon sequestration in maize-amended rice paddy soils. Sci Total Environ 458-460:319–330

Stone MM, DeForest JL, Plante AF (2014) Changes in extracellular enzyme activity and microbial community structure with soil depth at the Luquillo critical zone observatory. Soil Biol Biochem 75:237–247

Suárez-Abelenda M, Ahmad R, Camps-Arbestain M, Herath SHMSK (2015) Changes in the chemical composition of soil organic matter over time in the presence and absence of living roots: a pyrolysis GC/MS study. Plant Soil 391:161–177

Taube PS, Hansel FA, Madureira LA dos S, Teixeira WG (2013) Organic geochemical evaluation of organic acids to assess anthropogenic soil deposits of Central Amazon, Brazil. Org Geochem 58:96–106

Thevenot M, Dignac M-F, Rumpel C (2010) Fate of lignins in soils: a review. Soil Biol Biochem 42:1200–1211

Wanat N, Joussein E, Soubrand M, Lenain J-F (2014) Arsenic (As), antimony (Sb), and lead (Pb) availability from Au-mine Technosols: a case study of transfer to natural vegetation cover in temperate climates. Environ Geochem Health 36:783–795

Wiesenberg GLB, Schneckenberger K, Schwark L, Kuzyakov Y (2012) Use of molecular ratios to identify changes in fatty acid composition of Miscanthus × giganteus (Greef et Deu.) plant tissue, rhizosphere and root-free soil during a laboratory experiment. Org Geochem 46:1–11